First Detection of Extremely Enhanced Solar Wind Helium-3 Originated from the Lunar

X.Y. Wang [1], A.B. Zhang [2], L.G. Kong[3], S.Y. Zhang[4]

[1,2,3,4] National Space Science Center, Chinese Academy of Sciences；Key Laboratory of Environmental Space Detection；Beijing Key Laboratory of Space Environment Exploration,100190, China

Corresponding author: X.Y. Wang (orchard@nssc.ac.cn)

Key Points:

- The first observations of $_3He^{2+}$ density extremely enhanced to thousand times of average solar wind by SWID/Chang'E-2 is reported.
- Neutrals ionization and surface charging caused by energetic electrons induce $_3He$ losses from the lunar exosphere and may form ion voids.
- The loss of the exosphere and the formation of ionosphere ion void will be recurrent for the frequent energetic electrons injection.

Abstract

The first observations of $_3He^{2+}$ density extremely enhanced to thousand times of average solar wind by SWID/Chang'E-2 is reported in this paper. The two events occurred near the lunar and the Lagrange L2 point respectively. The synchronized energetic electrons increasing can induce the lunar surface charging to a large negative voltage and produce the electron-impact double ionization of helium-3 in the exosphere. $_3He^{2+}$ will converge to the lunar surface by the negative potentials, and fully pick up via non-resonance stochastic heating process by Alfvén wave of the solar wind. It indicates $_3He^{2+}$ in the events can originate from the lunar and transport to L2. Besides SEP (solar energetic events), the increasing of energetic electrons occurs frequently in quiet time, so the loss of the lunar exosphere will be recurrent, and the ionosphere ion void may be formed.

Plain Language Summary

Chang'E-2 is a lunar orbiter of launched in 2010. Solar wind ions are measured by SWIDs on board Chang’e-2.Helium-3 is one stable isotope of helium, which is expensive in earth because of its sparsity. The Solar wind Helium-3 from the sun inject and store in the lunar regolith. So there is abundant helium-3 in the lunar environment. It’s the first time we found the abnormal increase to thousands times of helium-3 ions in the solar wind when the Chang'E-2 is near the lunar and at the downstream of the lunar. Due to the scarcity of helium-3 on earth, it can be considered that the sun or the moon is its source. In the past, the observations of helium-3 enhancement in the solar wind originated from the sun have been reported. The enhancement can only reach 100 times. Our observations and researches show that the abnormal increasing of helium-3 originated from the moon rather than the sun, and can be increased to thousands times. These ions can move downstream far from the lunar. It will cause the ion void of the lunar ionosphere and the escape of lunar material.

1 Introduction

The photoionization, surface adsorption, and thermal escape are the primary loss mechanisms of the atomic species from the lunar exosphere (stern,1999; Killen and Ip, 1999;Wurz et al.2007). These loss processes are a relatively long and slow process. The rapid loss process and mechanism of the exosphere have not been reported. The moon has a tenuous exosphere and no intrinsic magnetic field. Helium is one of the main components in the lunar exosphere with surface densities of $2\sim7\times10^4/cm^3$ (Killen and Ip, 1999; Hodges, 1973, stern et al, 2012, Tirtha et al, 2017). Besides photoionization is regarded as the dominant loss process to helium, the double ionization of helium by the electrons impact can occur once the energy of the injected electrons comes up to 90.2eV (Shah, et al.1988). Lunar surfaces exposed to the ambient plasma, charged energetic particles, and UV radiation will become charged and develop a sheath with an electric field normal to the surface. Energy electron injections can induce the lunar surface charging to large negative potentials during SEP or BEE (Halekas, et al.2009; Wang, et al. 2012,2016). Newborn ions can be fully pickup by the solar wind Alfvén waves via the non-resonance stochastic heating process (Yoon and Wu, 1991; Wang et al. 2009, 2011, Sun et al. 2014; Liu et al. 2014). In the non-resonance stochastic heating process, ions are picked up by Alfvén wave in several gyro-periods and are heated in the process. The acceleration of low charge-to-mass will be more efficient. The ion velocity distribution becomes gradually isotropic when it catches up with Alfvén speed by stochastic heating. This means that ions in lunar space outside the sheath could be fully pickup by the solar wind in the presence of Alfvén waves. It has been previously observed that the ions picked up by the solar wind from the moon can form a partial or incomplete shell, and the phenomenon of fully pickup ions has not been observed.

Launched on Oct.1, 2010, Chang'E-2, as the second lunar orbiter of China, successfully entered a 100km altitude circular lunar orbit after a cislunar transfer trajectory and lunar capture phase. Then during a half-year flight in lunar orbit, Chang'E-2 completed the transfer to the Sun-Earth Lagrange L2 point and entered into the L2 point Lissajous orbit in August 2011 (Huang et al., 2012; Liu et al., 2014). On Chang'E-2, SWIDs and HPD are the backups of the instruments on Chang'E-1 (Wang et al. 2012; Kong et al.2011). SWIDs are designed to observe the 0.05~20keV/q solar wind ions, the energy sweep step is 48 with the resolution of 8.5% (FWHM). HPD is designed to observe the energetic charged particles respectively. SWID utilizes a typical top-hat electrostatic analyzer (ESA) with a fan-shaped field-of-view (FOV) of about 180°×6.7°. The ESA is separated into 12 apertures defined as C1 to C12. The HPD is outfitted with a sensor head composed of three silicon semiconductors. Before the flight, SWIDs were calibrated by the ion beam facility at IRAP (former CESR of Toulouse in France, Institut de Recherche en Astrophysique et Planétologie). HPD was calibrated on a tandem accelerator at CIAE (China Institute of Atomic Energy) and cyclotron at IMP (Institute of Modern Physics, Chinese Academy of Sciences).

On Oct.17, 2010, in the lunar orbit and on Sep.27, 2011, at the L2 point, solar wind $_3He^{2+}$ extreme enhancement and the 0.1~2MeV electrons increasing were almost synchronized observed by Chang'E-2. In this paper, we analyze the phenomenon and find that the most feasible origins of the extremely enhanced 3He2+ lie in the charged particles inducing surface charging and the ionization of the neutrals. Ions can concentrate on the surface by the sheath electric field and fully pickup by the Alfvén wave of the solar wind. This may lead to the rapid loss of helium in the lunar exosphere and the formation of ion void.

2 Observations

Distinct $_3He^{2+}$ fluxes peaks of solar wind ions observed by C12 of SWIDB on Oct.17, 2010, UT 11:00-12:00 (T1) and Sep.27, 2011, UT 10:45-12:40 (T2) are shown in Fig.1. And the other phenomenon as 0.1 ~ 2MeV electrons increase and solar wind 4He2+ acceleration were also observed in Fig.2-3. During T1, Chang'E-2 was in a polar orbit with an altitude of 90-120 km and was located at (-50.9RE, 37.6RE, 5.4RE)GSE on the lunar dayside and near side. In T2, Chang'E-2 moved to Lagrange-2 point, and the spacecraft traveled to (-243.2RE, 108.0RE, 7.0RE)GSE, downstream of the lunar. For the limited power source, the observation time interval of SWIDs on Sep.27, 2011, just lasted for 2 hours and 37 minutes. The solar incident angle between the symmetric axis of the measurement channel C12 and the Sun–Moon connection line is about 23º, as shown in Fig.1 (b3). Based on the model of the Earth's distant bow shock (Bennett et al. 1997), Chang'E-2 was in the solar wind on both T1 and T2. The schematic diagram in Fig. 1(a3), (b3) demonstrates the plasma regimes and the observation geometry of SWIDB in aberrated GSE coordinate. The longitude, latitude, and altitude of Chang'E-2 in the selenocentric solar ecliptic (SSE) coordinate system of T1 are shown in Fig,1 (a4).

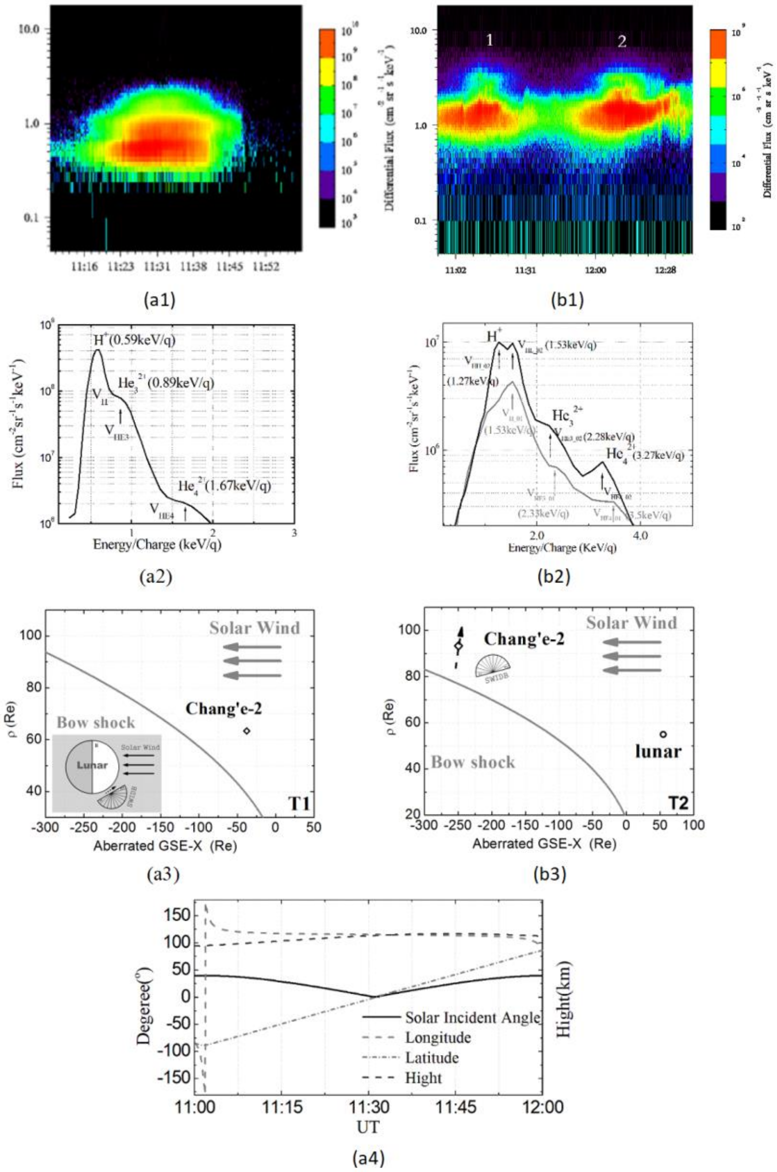

Figure 1. Observations of solar wind fluxes peaks spectrum of H^+, $_3He^{2+}$, $_4He^{2+}$ at UT 2010-10-17 11:00-12:00 (T1, a1-a4) and UT 2011-9-27 10:55-12:40 (T2, b1-b3) by C12 of SWIDB. (a1, b1) the time-energy spectrogram of solar wind ions in T1 and T2. The vertical coordinate is Energy/Charge and the horizontal is universal time. (a2, b2) the energy-fluxes profiles of Solar wind ion in T1 and T2. The subscript 01 and 02 in (b1) identify the sequential number for the periodical precession of Chang'E-2. (a3, b3) the observation geometry of SWIDB and the location of the spacecraft during T1 and T2, (a4) the solar incident angle of C12, longitude, latitude, and altitude of the Chang'E-2 in selenocentric solar ecliptic (SSE) coordinate system in T1.

2.1 Extreme Enhancement of $^3He^{++}$ in the solar wind (EEH)

The obvious differential flux peaks of H^+, $_3He^{2+}$, and $_4He^{2+}$ are shown in Fig.1 (a2) and Fig.1 (b2) and are signified by arrows. There are one proton beam and two alpha beams of $_3He^{2+}$ and $_4He^{2+}$ in Fig.1 (a2) and the first period of Fig.1 (b2). But two proton beams and two alpha beams of $_3He^{2+}$ and $_4He^{2+}$ exist in the second period in Fig.1 (b2). The bulk speed of H^+, $_3He^{2+}$, and $_4He^{2+}$ beams are defined as V_H, V_{HE3}, and V_{HE4} in Fig. 1(a2). In Fig. 1(b2), V_{H_01}, V_{HE3_01}, and V_{HE4_01} flux peaks in the gray line of the first period indicate the bulk speed of H^+, $_3He^{2+}$, and

$_4He^{2+}$ beams. The H^+ beams and two alpha beams of $_3He^{2+}$ and $_4He^{2+}$ are referred to as V_{HL_02}, V_{HH_02}, V_{HE3_02}, and V_{HE4_02} in the second period with the black line.

The penultimate particle peak is verified as $_3He^{2+}$ because of the M/Q=1.5 amu/e in Fig1. The 1-8 orbits H^+ and $_4He^{2+}$ observation result from 0:00-16:00 UT on 2010-10-17 around T1 (the 6th orbit) was shown in Fig 2. In Fig2(c), the peak of the last particle is verified as $_4He^{2+}$ because the M/Q=2 amu/e on 1-3th orbits. $_4He^{2+}$ velocity is divided by $(M_{He4}/Q_{He4})^{1/2}= (2)^{1/2}$ and $_3He^{2+}$ velocity is divided by $(M_{He3}/Q_{He3})^{1/2}= (1.5)^{1/2}$. In Fig2. (b), the $_4He^{2+}$ acceleration and moderated to the proton P1 speed is observed. In T1, the ratio of Energy/Charge between the first two peaks of H^+, $_3He^{2+}$ is factor 1:1.5 with the V_H and V_{HE3} of ~336km/s. The solar wind bulk speed by ACE/SWEPAM is ~331km/s as V_H in T1 through a time shift method of about 1h delay. Moreover, the V_{HE4} for $_4He^{2+}$ of ~400km/s approximates 64 km/s higher than the V_H and V_{HE3}. In the two periods of T2, the FOV of C12 is derived from the solar wind center of about 23 °. For the first period, the ratio of Energy/Charge between the proton peak and $_3He^{2+}$ peak is factor 1.5:2 with the V_{H_01} and V_{HE3_01} of ~541km/s, while the V_{HE4_01} for $_4He^{2+}$ of ~570km/s approximates 29km/s higher than the V_{HE3_01} and V_{H_01}. During this period, the average solar wind bulk speed is ~600km/s by ACE/SWEPAM through a time shift method of about 1.5h delay. In the second period, the Energy/Charge of the middle two peaks of high-speed H^+ and $_3He^{2+}$ is factor 1:1.5 with the V_{HH_02}, and V_{HE3_02} of ~540km/s, which exceeds the low-speed proton beam's velocity V_{HL_01} of ~493km/s by about 57 km/s. The V_{HE4_02} for $_4He^{2+}$ of ~560km/s approximates 20 km/s higher than the V_{HE3_02} and V_{HH_02}. For this period, the average solar wind bulk speed is ~567km/s by ACE/SWEPAM.

We calculate the ratio of phase space density for $_4He^{2+}/H$, $_3He^{2+}/H$, and $_3He^{2+}/_4He^{2+}$ during these two events. The $_4He^{2+}/H$ ratio is ～0.01. It is similar to the average solar wind value. The $_3He^{2+}/H$ ratio is ～0.03 and $_3He^{2+}/_4He^{2+}$ ratio is ～3. $_3He^{2+}/_4He^{2+}$ ratio equating to about 6000 times the average solar wind value of $\sim 4.9\times10^{-4}$ (Ansgar et. al 2008; Robert et al.,2002; P. Bochsler et al.,1990; George et al. 1998). In T1, the minimum solar incident angle is about 0^o, and the density of $_3He^{2+}$ is ～$0.01cm^{-3}$. Thus, we call these performances as Extreme Enhancement of $_3He^{2+}$ events (EEH).

In T1 and T2, the thermal speed/solar wind speed is ~0.15 and ~0.14 separately. Despite the different solar wind conditions for the two EEH, the core distribution of the thermal is broad. And no obvious $_4He^+$observed in these events.

2.2 The turbulence of the space environment

The weekly highlights of Space Weather Prediction Center (SWPC) reported that a transient-like feature was observed at ACE on October 17 between 0111 UTC and 1150 UTC as Bz went through an extended negative period. The peak negative values around -7nT when a possible source of the slow CME was observed on October 14. And a group of super-thermal ions from UT01:20 to 06:10 were observed simultaneously by Chang'E-2 at 1-3th orbit in Fig.2 (a). The bulk speed variations of the protons and $_4He^{2+}$ are unveiled in Fig.2 (b). $_4He^{2+}$ acceleration is commencing on the 4th orbit. The difference of bulk velocity between the proton beam and $_4He^{2+}$ beam was 34-110km/s in 4-6 orbit. In Fig.2 (a), the acceleration of the ions occurred at 10:10 and lasted until the FOV of C12 was far from the solar wind center. The ions' central energy increased at least 0.4keV in 20 minutes. The EEH of T1 that occurred in the 6th orbit is mentioned in section 2.1. The energy-fluxes profiles of the protons and $_4He^{2+}$ in 4, 5, 7th orbit can be seen from Fig.2(c). In the 5th orbit, the energy-fluxes profiles broadened in the polar direction, the total flux increased and the temperature does not change significantly. The double proton beams for P1 and P2 arose in the 7th orbit. The bulk speed of P2 in sync with $_4He^{2+}$ and the velocity difference between the two proton beams is ~66km/s. In the 8th orbit, the solar wind proton beam reverted to a single peak with the coincidence of bulk speed of $_4He^{2+}$ and proton.

A SEP began on Sep. 23, 2011, was reported by SWPC and observed by HPD. In Fig3.(b), the flux peaks of >10MeV protons reached to 40 $(cm^2 \cdot sr \cdot s \cdot MeV)^{-1}$. For T2, an ICME without the magnetic cloud, starting from 20:00 on Sep.26 and ending at 15:00 on Sep.28, was publicized in the ICME tables list by Richardson and Cane (http://www.srl. caltech.edu/ACE/ ASC/DATA/level3/icmetable2.htm). During T2, the obvious acceleration of ions was observed at 12:22~12:32 in Fig.1 (b1) and Fig.3 (d). The ions sustained acceleration until the FOV of the C12 far from the solar wind center, and the peak energy of the ions increased ~0.46keV.

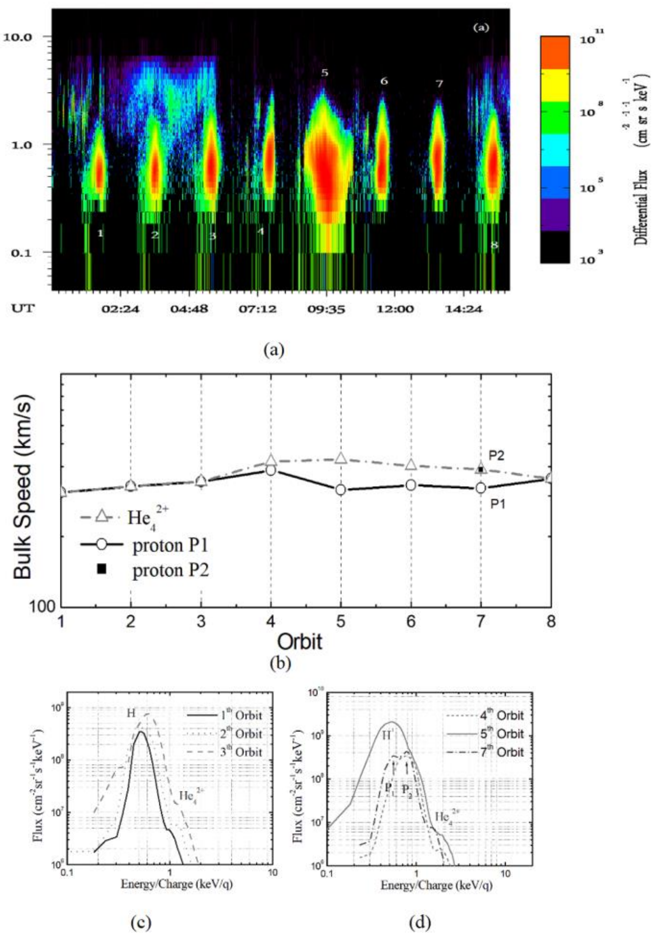

Figure 2. The observation result of C12 measurement channel of SWID-B from 0:00-16:00 UT on 2010-10-17. 1-8 is the sequential number for Chang'E-2 orbiting the lunar and indicates the spacecraft orbits the lunar for 8 times. (a) Energy/Charge-Time spectrogram of C12. (b) The bulk speed of the solar wind $_4He^{2+}$ and protons in each of the orbits. The curve with circles, squares, and triangles are the bulk speed of protons and $_4He^{2+}$. P1 and P2 show the velocity of double proton beams in the 7th orbit. (c) Energy/Charge-Fluxes profiles of Solar wind ions in 1, 2, 3rd orbit. (c) Energy/Charge-Fluxes profiles of Solar wind ions in 4, 5, 7th orbit.

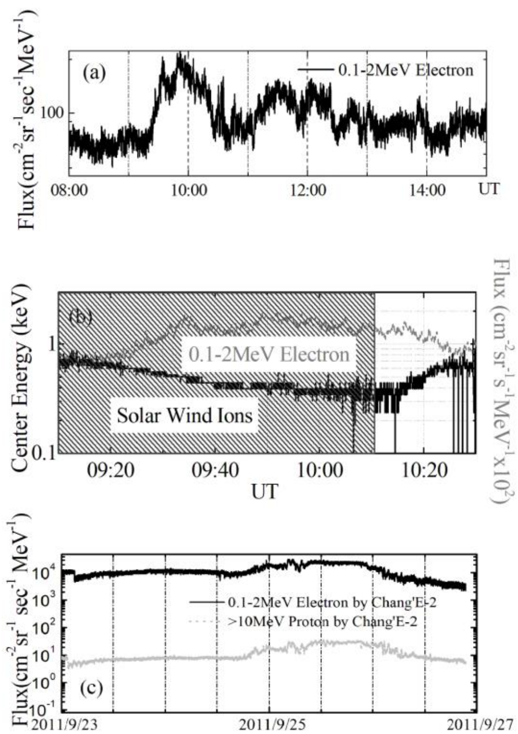

Figure 3. 0.1-2.0MeV keV energetic electrons increase and the acceleration of solar wind ions observed by HPD/Chang'E-2. (a) The rising of the energetic electrons manifests a BEE event that occurred on 2010-10-17 9:17 and lasted for about 5 hours. (b) In the 5th orbit on 2010-10-17, the 0.1-2.0MeV electron fluxes peaked at 9:50 and subsequently increased at least 0.4keV of the ions' central energy. (c) The fluxes of energetic electrons increased greatly during SEP on 2011-9-23 16:00 ~2011-9-27 16:00. (d) The peak energy of the ions increased ~0.46keV on 2011-9-27 12:26~12:36.

2.3 Increasing of Energetic electrons and lunar surface charging

The rise of 0.1-2.0MeV energetic electrons was observed by HPD/Chang'E-2 during the two EEH in Fig3. In T1, the bursting of the energetic electrons indicated the occurrence of a BEE event (Wang et al. 2012, 2011). The energetic electrons during BEE are directional obviously. However, in T2, the fluxes of energetic electrons surged is due to the solar energetic events (SEP). The general magnitude of the ubiquitous background 0.1~2.0MeV electrons fluxes observed by HPD was ~10^1(cm^2·sr·s·MeV)$^{-1}$. On Oct.17, 2010, 9:17 UT, 0.1~2.0MeV energetic electrons injected impulsively in Fig.3 (a) and sustained high flux for about 5 hours with the flux peaks reaching the magnitude of ~10^2 (cm^2 ·sr·s·MeV)$^{-1}$. For T2, the 0.1~2.0MeV energetic electrons injected sustained high flux with the peak fluxes reaching the magnitude of ~10^4 (cm^2 · sr· s ·MeV)$^{-1}$.

The increasing of energetic electrons suggested the EEHs were subsequent with the lunar and spacecraft surface charging. Wang et al. (2012, 2016) demonstrated that BEE can induce circumlunar spacecraft and the lunar surface charging to negative kilovolts when the temporal integral of the energetic electrons fluxes exceeds 10^{11} cm^{-2}. And the charging process is sustained for the same interval as the BEE. For T1, we calculated the surface potentials of the lunar utilizing the simulation method by Wang et al. (2012, 2016). The calculation result shows that the temporal integral of the electrons fluxes can reach up to >10^{11} cm^{-2} and the lunar surface charging voltage can reach up to more than –0.75kV. The result is consistent with the magnitude of at least 0.4keV increase of solar wind ions energy as mentioned in section 2.2. For the lunar surface potentials is much more negative than kT_e/e, an ion matrix or transient sheath forms around the surface and expands to the solar wind. The total sheath thickness (S_C) can be obtained from the quasistatic Child–Langmuir law

$$S_C = \frac{\sqrt{2}}{3}\left(\frac{2eU_0}{kT_e}\right)^{3/4}\lambda_D.$$

In the above expressions, λ_D is the Debye length, *T*e is the electron temperature, U_0 is negative surface bias. According to the above formula, sheath thickness S_C is at least 30 meters.

For T2, SEP occurred with the fluxes of 0.1~2MeV electrons reaching to >10^3 (cm^2 ·sr·s·MeV)$^{-1}$ and sustained for more than 4 days from Sep.23, 2011, to Sep.27, 2011. Halekas et al. (2009) proposed that the spacecraft and lunar surface potentials can reach negative kilovolts values during SEP. This indicates that in T2, the lunar surface charging potentials can reach up to a large negative voltage. It was confirmed by the 0.46keV increment of ion energy in section 2.2. So the lunar surface potentials amplitude of variations can reach up to -0.46kV.

3 Origin, ionization, and pickup of $_3He^{2+}$ in EEHs

3.1 The origin of $_3He^2$ enhancements

The abnormal increase of helium-3 in the two EEHs can originate from the sun or the moon. In these events, $_3He^{2+}$/$^4He^{2+}$ ratios elevated by a factor of 6000 exceedingly surpass those in early reports of keV $_3He^{2+}$ enhancement events (EHs) in the solar wind. In EHs, the factors are 4~100 than those in the average solar wind (Ho, 1998; Gloeckler, 1999; Wittenberg, 2000). The EHs are associated with CME passage and $_3He^{2+}$ stems from the solar. Most of the EHs were within or trailing the magnetic clouds. An overabundant $_4He^+$ was observed in these EHs. It implied that because of the expansion and cooling of the CME transit from the Sun, the temperature in EHs is much lower than (<10^5 K) the typical million-degree freeze observed in the normal solar wind. However, an ICME without magnetic cloud was reported during T2 and none of the ICME occurred during T1. Unlike EHs, none of the noticeable $_4He^+$ was observed in EEHs. The temperature is of ~2×10^5 K in T1 and ~3×10^5 K in T2 confirmed that the core distributions of the thermal plasma are not as narrow as in CME. Extra high fluxes of $_3He^{2+}$ ions, the absence of $^4He^+$, and high kinetic temperature suggest the different origins of solar wind $_3He^{2+}$ enhancements between the EHs and EEHs.

In addition to the origin of the sun, there are two mechanisms of the lunar origins. The first is from the helium ionization of the lunar exosphere. Since the majority of the lunar exosphere Helium is of the solar wind origin, it is known to scale with the solar wind alpha particle flux (Hurley et a., 2016). The diurnal variation of Helium is at around ∼2×10^3/cm^2 to ~4×10^4/cm^2 (Hodges, 1975). CHACE/MIP /Chandrayaan-1 evidenced that the upper limit of neutral helium density can reach 8×10^2/cm^2 in the sunlit when the Helium abundance in the Moon had hit one of its lowest values (Tirtha et al., 2017). Because of the observations of Helium rich solar wind in two EEHs, we assume that the concentration of helium in the exosphere can reach the magnitude of 10^2 ~10^4/cm^2. The double ionization of helium-3 can occur once the energy of the injected electrons >90.2eV. The cross section is ~10^{-20} cm^2 for the helium double ionized by >1keV electrons (Shah et al. 1998). The trend of surface charge to negative potentials is consistent with that of energetic electron increasing. Combined with the average ^3He/^4He ratio, the total amount of double ionized $_3He^{2+}$ in the sheath with a thickness of 30 meters and an area of 1 cm^2 is around 0.0002~0.02. The produced ions will converge to the lunar surface in the negative sheath electric field. Since the lunar regolith is an electrical insulator, deposited charged particles can remain in the lunar surface regolith for prolonged intervals. When the lunar surface potential is reversed, the ions deposited on the surface will be modulated by the solar wind electromagnetic field and pick up by the solar wind.

There is another possible loss mechanism by energetic particles penetrate the lunar regolith cause deep dielectric charging and breakdown(Jordan et al. 2014, 2019). Campins and Krider's experiments suggest that dielectric breakdown can melt and boil off material. The breakdown can occur when the difference in fluxes between protons and electrons is at least $\sim 10^{10}$ cm−2. It can be derived that the helium-3 released from the area of 1cm2 is about several to hundreds of particles in the two EEHs. According to the collision cross section, the ionized helium-3 is much lower than the observations in the EEHs. Therefore, the deep dielectric charging and breakdown in lunar regolith is not enough to comprehend the abnormal increase of helium-3 in the solar wind. These results indicate that the primary source of abnormal helium 3 in this paper should be the ionization of the exosphere.

3.2 ${}_{3}He^{2+}$ ions fully pickup by the solar wind

The double proton beams and the acceleration of the solar wind helium ions mentioned in sections 2.1-2.2 suggested the existence of Alfvén wave during T1 and T2. For T1, The IMF |B| value for the orbit 4-7th in Fig.2 is 5-10nT from ACE by the time-shift method and the solar wind density is 3.0cm^{-3} by Chang'E-2. Accordingly, the local Alfvén velocity was calculated as 63~126km/s. It is almost consistent with the variation of velocity difference between the ${}_{4}He^{2+}$ and proton P1 in Fig.2 (b). For the orbit 2-3th, the difference between the center speed of the super-thermal ions and the bulk speed of the proton in Fig.2 (a) was ~120km/s. In the 7th orbit, the high- speed proton beam P2 appeared with the same speed as ${}_{4}He^{2+}$. Then in the 8th orbit, the single proton beam recovered with the same velocity as ${}_{4}He^{2+}$. It suggests that the Alfvén wave has existed in the solar wind for more than 3 hours before T1. Although the resonance conditions were not satisfied because the initial bulk speed of ${}_{3}He^{2+}$ is of ~0, ${}_{3}He^{2+}$ ions can be picked up by the solar wind via non-resonance interaction and sustaining stochastic heating due to the existence of the Alfvén wave. It is generally known that solar wind Alfvén waves originate from the sun. Solar wind proton and helium-4 were accelerated by Alfvén wave except for helium-3 ions, which suggests that helium-3 is not originating from the solar.

For T2, the spacecraft was located in the solar wind downstream distant to the lunar. Although the FOV has deviated from the solar wind center, the ${}_{3}He^{2+}$ and ${}_{4}He^{2+}$ beams of ~57 km/s and ~25 km/s higher than the low-speed proton beam's velocity were observed in the two periods respectively. It is indicating the existence of Alfvén wave and consistent with the non-resonance stochastic heating process, where the velocity of the solar wind pickup ions will increase by an Alfvén speed after enough time.

4 Discussion and conclusions

Two extreme enhancements of ${}_{3}He^{2+}$ by thousands of times average solar wind value and the 0.1~2MeV electrons bursting are observed by SWIDs and HPD when Chang'E-2 orbits around the moon and at L2 point in the solar wind. The two EEHs occurred when the spacecraft was in the solar wind around the lunar and the lunar downstream respectively. The difference from EHs indicates the helium-3 in EEHs is not originated from the sun. Both the lunar exosphere and lunar regolith are rich in helium, the lunar should be the potential candidate to be the provenance. The dielectric breakdown caused by energetic particles penetrates the lunar regolith can release outgases to the exosphere. Double ionization of helium-3 will occur by the >90.2eV energetic electrons injection. Energetic electrons increasing can induce the lunar surface charging to negative kilovolts in the sheath of >30 meters. The ions in the sheath will converge to the surface by the electric field. When the lunar surface potential is reversed, the ${}_3He^{2+}$ ions distributed on the lunar surface will be pickup by the turbulent solar wind alternatively. The speed difference of the solar wind proton and helium beams in both EEHs identified the existence of Alfvén wave. Helium-3 deriving from the lunar can be fully picked up by the solar wind in the non-resonance stochastic heating process and traveling downstream to L2 point. In the two events, the calculation shows that helium-3 produced by dielectric breakdown is much lower than in EEHs. The maximum surface density for ${}_3He^{2+}$ produced in the exosphere can reach 0.02 cm^{-2}. So the primary lunar source of solar wind abnormal helium-3 in the two EEHs should be the lunar exosphere.

In this paper, we find only two EEHs, which is much lower than the probability of BEE. Firstly, the SWIDs were unable to distinguish M/Q in the isotropic plasma; secondly, the different processes of ions with diverse mass numbers or charges, such as the acceleration by the electric field, and the non-resonance stochastic heating process, leading to their fractionation. And for the lack of magnetic field data, it’s difficult to deduce the exact local positions of the Helium-3 deriving from the lunar or to confirm the concrete pickup process. The results indicate the occurrence of ions void in the lunar exosphere. Since the frequent occurrence of BEEs can lead the surface charging to large negative potentials and the neutrals ionizing, the phenomenon of ion void in the exosphere will be recurrent. It will cause the instability of the lunar ionosphere and the loss of lunar material. Moreover, because the lunar surface potentials can be charged to large negative potentials and last a long time during SEP, the speculation can be made that the neutrals ionizing and loss in the lunar exosphere could arise frequently in the high-level solar activity period.

Future more, the detection of the electromagnetic field, neutrals, and charged particles on the following Chang’E series could offer us the chance to evidence the effects of energetic electron injection in the lunar space environment and verify the lunar Ionospheric disturbances.

Acknowledgments

Our gratitude goes to all the members of SWIDs and HPD work team. We appreciate Professor Henri Reme for providing us with the opportunity to calibrate the SWIDs at Centre d’Etude Spatiale des Tayonnements in Toulouse, France. We feel grateful to the ACE team to provide the solar wind plasma and IMF data. We thank Professor Li Hui, and Chen Tao for their helpful suggestions. This research is supported by the Strategic Priority Research Program of Chinese Academy of Sciences (Grant No. XDA17010303， XDA04077100) and National Science Foundation of China (NSFC, Grant NO. 41204128). Chang’E-2 used in this paper, which is available at http://moon.bao.ac.cn/searchOrder_pdsData.search. ACE data is available at http://www.srl.caltech.edu/ACE/ASC/index.htm.

References

Deng, A., & Stauffer, D. R. (2006), On improving 4-km mesoscale model simulations. *Journal of Applied Meteorology and Climatology*, *45*(3), 361–381. doi:10.1175/JAM2341.1

Ansgar Grimberg, Heinrich Baur, Fritz Buhler, Peter Bochsler, & Rainer Wieler. (2008), Solar wind helium, neon and argon isotopic and elemental composition: Data from the metallic glass flown on NASA’s Genesis mission. *Geochimica et Comsmochimica Acta.*,72, 626-645

Stern S A., (1999),The lunar atmosphere: history, status, current problems, and context. *Reviews of Geophysics*, 37:453-491

Bennett L., Kivelson M. G., Khurana K. K., Frank L.A., & Paterson W.R., (1997), A model of the Earth's distant bow shock. *Journal of Geophysical Research*, 102 (A12), 26927-26941

Bochsler P., Geiss J., & Maeder A., (1990), The abundance of 3He in the solar wind a constraint for models of solar evolution, *Solar physics*. 128,203-215

Campins, H., & E. P. Krider. (1989), Surface discharges on natural dielectrics in the solar system, *Science*, 245, 622–624, doi:10.1126/ science.245.4918.622

George Gloeckler, & Johannes Geiss, (1998), Measurement of the abundance of helium-3 in the sun and in the local interstellar cloud with SWICS on ULYSSES. *Space Science Reviews*, 84:275-284

Gloeckler G., Fisk L. A., Hefti S., Schwadron N. A., Ipavich, T.F. M. Geiss J., et al., (1999), Unusual composition of the solar wind in the 2-3 May 1998 CME， observed with SWICS on ACE. *Geophy. Res. Lett*. 26(2), 157-160

Halekas, J. S., Delory G. T., Lin R. P., Stubbs T. J., & Farrell W. M. (2009), Lunar surface charging during solar energetic particle events: Measurement and prediction. *J. Geo. Res. Let.*, 114, A05110

Hurley, D.M., Cook, J.C., Benna, M., Halekas, J.S., Feldman, P.D., Retherford, K.D., et al., (2016), Understanding temporal and spatial variability of the lunar helium atmosphere using simulta- neous observations from LRO, LADEE, and ARTEMIS. *Icarus*, 273, 45–52

Ho, C. W. (1998), Helium-3 enhancements and unusual ion charge state composition in coronal mass ejections. *University of Maryland College Park*.

Hodges R.R., & JR, J., (1973), Helium and Hydrogen in the Lunar Atmosphere, *Geo. Res.*, 78(34), 8055-8064

Hodges, R.R., (1975), Formation of the lunar atmosphere. *Moon*, 14, 139–157

Huang H., (2012), chang’e-2 satellite Lagrange L2 point Mission. *63th International astronautical Congress*, Naples, Italy

Jordan A. P., Stubbs T. J., Wilson J. K., Schwadron N. A., Spence H. E., Joyce C. J., (2014), Deep dielectric charging of regolith within the Moon’s permanently shadowed regions, *J. Geophys. Res. Planets*, 119, 1806–1821

Jordan A. P., Stubbs T. J., Shusterman M.L.， Izenberg N.R.,Wilson J. K., Hayne P.O. et al, (2019), How dielectric breakdown may contribute to the global weathering of regolith on the moon， *Icarus*, 319, 785–794

Killen R., & Ip W.H., (1999), The surface-bounded atmospheres of Mercury and the Moon, *Rev. Geophys.* 37(3), 361-406 .

Kong L. G., Wang S. J., Wang X. Y., Zhang A.B., Zhu G.W., Yu D.J. et al., (2011), In-flight Performance and Preliminary Observational Results of Solar Wind Ion Detectors (SWIDs) on Chang'E-1. *Planetary and space Science*, 62(1),23-30.

Liu H. F., Wang S. Q., Li K. H., & Tang C. J., (2014), Nonresonant and stochastic heating of ions by low-frequency wave. *Physics Letters*, A. 378, 3614–3616

Liu L., Liu Y., Cao J. F., Hu S.J. Tang G.S. & Xie J. F., (2014), Chang'e-2 lunar escape maneuvers to the sun-Earth L2 libration point mission. *Acta Astronautica*., 93, 390-399

Robert F.Wimmer-Schweingruber. (2002),The composition of the solar wind. *Adv Space Res.*, 30(1),23-32

Shah M. B., Elliott D. S., McCallion P., & Gibody H. B., (1988), Single and double ionization of helium by electron impact, *J. Phys. B: At. Mol. Opt. Phys.*, 21, 2751-2761

Stern, S.A., Retherford, K.D., Tsang, C.C.C., Feldman, P.D., Pryor, W., & Gladstone, G.R., (2012), Lunar atmospheric helium detections by the LAMP UV spectrograph on the Lunar Reconnaissance Orbiter. *Geophys. Res. Lett.*, 39, L12202. doi:10.1029/2012GL051797.

Sun J. C., Gao X. L., Lu Q. M., & Wang S., (2014), The Efficiency of Ion Stochastic Heating by a Monochromatic Obliquely Propagating Low-Frequency Alfven Wave. *Plasma Science and Technology*, 16(10)

Tirtha P. D., Thampi S. V., Dhanya M.B., Anil B., Ahmed S.M., & Sridharan R., (2017), Upper limit of helium-4 in the sunlit lunar exosphere during magnetotail passage under low solar wind condition: Result from CHACE aboard MIP in Chandrayaan-1, *Icaru* , 297, 189–194

Wang B., & Wang C. B., (2009), Heating rate of ions via nonresonant interaction with turbulent Alfvén waves with ionization and recombination. *Physics of plasmas*, 16, 082902

Wang B., Wang C. B., Yoon P. H., & Wu C. S., (2011), Stochastic heating and acceleration of minor ions by Alfvén waves. *Geophy. Res. Lett.*, 38, L10103, doi: 10.1029/2011GL047729

Wang X. Y., Zhang A. B., Zhang X.G., Reme H., Kong L.G., Zhang S.Y. et al., (2012), Bursts of Energetic Electron Induced Large Surface Charging Observed by Chang'E-1. *Planetary and space science*, 71(1), 1-8

Wang X. Y., Zhang A. B., Jing T., Reme H., Kong L. G., Zhang S. Y., et al., (2016), Synchronization of Energetic Electrons Bursting and the Lunar Orbiter Surface Charging to negative Kilovolts. *Chinese J. Geophys.*, 59(10), doi: 106038/cjg20161001, 2016

Wittenberg E., Hjections L.， George C.H., Douglas C.Hamilton, George Gloeckler, & Peter Bochsle. (2000), Enhanced Solar Wind 3He2+Associated with Coronal Mass, *Geophy. Res. Lett.*, 27 (3), 309-312

Wurz P., Rohner U., Whitby J.A., Kolb C., Lammer H., Dobnikar P. et al., (2007), The lunar exosphere: The sputtering contribution, *Icarus*, 191,486-496

Yoon P. H., & Wu C. S., (1991), Ion Pickup by The Solar Wind Via Wave-particle Interactions. *American Geophysical Union*, 61, 241-258